UNITED NATIONS EDUCATIONAL, SCIENTIFIC AND CULTURAL ORGANIZATION
INTERNATIONAL ATOMIC ENERGY AGENCY
INTERNATIONAL CENTRE FOR THEORETICAL PHYSICS
I.C.T.P., P.O. BOX 586, 34100 TRIESTE, ITALY, CABLE: CENTRATOM TRIESTE

SMR/1006 - 34

COURSE ON "OCEAN-ATMOSPHERE INTERACTIONS IN THE TROPICS"
26 May - 6 June 1997

Articles

"After the Deluge: Mediterranean Stagnation & Sapropel Formation"

&

"African Monsoons, an Immediate Climate Response to Orbital Insolation"

presented by

N. Pinardi
IMGA/CNR
Bologna
Italy

Please note: These are preliminary notes intended for internal distribution only.

16. Brown, D. D. & Sugimoto, K. *Cold Spring Harb. Symp. quant. Biol.* **38**, 501–505 (1973).
17. Wegnez, M., Monier, R. & Denis, H. *FEBS Lett.* **25**, 13–20 (1972).
18. Ford, P. J. & Southern, E. M. *Nature new Biol.* **241**, 7–12 (1973).
19. Ford, P. J. & Brown, R. D. *Cell* **8**, 485–493 (1976).
20. Parker, C. S. & Roeder, R. G. *Proc. natn. Acad. Sci. U.S.A.* **74**, 44–48 (1977).
21. Pelham, H. R. B., Wormington, W. M. & Brown, D. D. *Proc. natn. Acad. Sci. U.S.A.* **78**, 1760–1764 (1981).
22. Pelham, H. R. B., Bogenhagen, D. F., Sakonju, S., Wormington, W. M. & Brown, D. D. *ICN-UCLA Symp.* (in the press).
23. Korn, L. J. & Brown, D. D. *Cell* **15**, 1145–1156 (1978).
24. Fedoroff, N. V. *Cell* **16**, 551–563 (1979).
25. Pribnow, D. *Proc. natn. Acad. Sci. U.S.A.* **72**, 784–788 (1975).
26. Gilbert, W. in *RNA Polymerase* (eds Losick, R. & Chamberlin, M.) 193–205 (Cold Spring Harbor Laboratory, New York, 1976).
27. Brown, K. D., Bennett, G. N., Lee, F., Schweingruber, M. F. & Yanofsky, C. *J. molec. Biol.* **121**, 153–177 (1978).
28. Rosenberg, M. & Court, D. *A. Rev. Genet.* **13**, 319–353 (1979).
29. Sakonju, S., Bogenhagen, D. F. & Brown, D. D. *Cell* **19**, 13–25 (1980).
30. Bogenhagen, D. F., Sakonju, S. & Brown, D. D. *Cell* **19**, 27–35 (1980).
31. Wormington, W. M., Bogenhagen, D. F., Jordan, E. & Brown, D. D. *Cell* **24**, 809–817 (1981).
32. Thimmappaya, B., Jones, N. & Shenk, T. *Cell* **18**, 947–954 (1979).
33. Fowlkes, D. M. & Shenk, T. *Cell* **22**, 405–413 (1980).
34. Roeder, R. G. in *RNA Polymerase* (eds Losick, R. & Chamberlin, M.) 285–329 (Cold Spring Harbor Laboratory, New York, 1976).
35. Engelke, D. R., Ng, S. Y., Shastry, B. S. & Roeder, R. G. *Cell* **19**, 717–728 (1980).
36. Roeder, R. G. *et al. ICN-UCLA Symp.* **14**, 521–540 (1979).
37. Honda, B. M. & Roeder, R. G. *Cell* **22**, 119–126 (1980).
38. Sakonju, S. *et al. Cell* **23**, 665–669 (1981).
39. Kay, B. K., Schmidt, O. & Gall, J. G. *J. Cell Biol.* **90**, 323–331 (1981).
40. Telford, J. L. *et al. Proc. natn. Acad. Sci. U.S.A.* **76**, 2590–2594 (1979).
41. DeFranco, D., Schmidt, O. & Söll, D. *Proc. natn. Acad. Sci. U.S.A.* **77**, 3365–3368 (1980).
42. Hagenbüchle, O., Larson, D., Hall, G. I. & Sprague, K. U. *Cell* **18**, 1217–1229 (1979).
43. Sprague, K. U., Larson, D. & Morton, D. *Cell* **22**, 171–178 (1980).
44. Garber, R. L. & Gage, L. P. *Cell* **18**, 817–828 (1979).
45. Kressmann, A., Hofstetter, H., DiCapua, E., Grosschedl, R. & Birnstiel, M. L. *Nucleic Acids Res.* **7**, 1749–1763 (1979).
46. Koski, R. A., Clarkson, S. G., Kurjan, J., Hall, B. D. & Smith, M. *Cell* **22**, 415–425 (1980).
47. Brown, R. D. & Brown, D. D. *J. molec. Biol.* **102**, 1–14 (1976).
48. Bogenhagen, D. F. & Brown, D. D. *Cell* **24**, 261–270 (1981).
49. Korn, L. J., Queen, C. L. & Wegman, M. N. *Proc. natn. Acad. Sci. U.S.A.* **74**, 4401–4405 (1977).
50. Adhya, S. & Gottesman, M. *A. Rev. Biochem.* **47**, 967–996 (1978).
51. Brown, D. D. & Sugimoto, K. *J. molec. Biol.* **78**, 397–415 (1973).
52. Peterson, R. C., Doering, J. L. & Brown, D. D. *Cell* **20**, 131–141 (1980).
53. Brown, D. D. & Weber, C. S. *J. molec. Biol.* **34**, 661–680 (1968).
54. Brown, D. D. & Dawid, I. B. *Science* **160**, 272–280 (1968).
55. Dawid, I. B., Brown, D. D. & Reeder, R. H. *J. molec. Biol.* **51**, 341–360 (1970).
56. Gall, J. G. *Proc. natn. Acad. Sci. U.S.A.* **60**, 553–560 (1968).
57. Perkowska, E., MacGregor, H. L. & Birnstiel, M. L. *Nature* **217**, 649–650 (1968).
58. Brown, D. D. & Blackler, A. W. *J. molec. Biol.* **63**, 75–83 (1972).
59. Brown, D. D. & Littna, E. *J. molec. Biol.* **20**, 95–112 (1966).
60. Miller, L. *Cell* **3**, 275–281 (1974).
61. Pelham, H. R. B. & Brown, D. D. *Proc. natn. Acad. Sci. U.S.A.* **77**, 4170–4174 (1980).
62. Picard, B. & Wegnez, M. *Proc. natn. Acad. Sci. U.S.A.* **76**, 241–245 (1979).
63. Sakonju, S. thesis, Johns Hopkins Univ.
64. Korn, L. J. & Gurdon, J. B. *Nature* **289**, 461–465 (1981).
65. Pardue, M. L., Brown, D. D. & Birnstiel, M. L. *Chromosoma* **42**, 191–203 (1973).
66. Ford, P. J. & Mathieson, T. *Nature* **261**, 433–435 (1976).
67. Brown, D. D., Carroll, D. & Brown, R. D. *Cell* **12**, 1045–1056 (1977).
68. Fedoroff, N. V. & Brown, D. D. *Cell* **13**, 701–716 (1978).
69. Carroll, D. & Brown, D. D. *Cell* **7**, 467–475 (1976).
70. Carroll, D. & Brown, D. D. *Cell* **7**, 477–486 (1976).
71. Fedoroff, N. V. *Cell* **16**, 697–710 (1979).
72. Brown, D. D., Wensink, P. C. & Jordan, E. *Proc. natn. Acad. Sci. U.S.A.* **68**, 3175–3179 (1971).
73. Brownlee, G. G., Cartwright, E., McShane, T. & Williamson, R. *FEBS Lett.* **25**, 8–12 (1972).
74. Fedoroff, N. V. & Brown, D. D. *Cold Spring Harbor Symp. quant. Biol.* **42**, 1195–1200 (1977).
75. Miller, J. R., Cartwright, E. M., Brownlee, G. G., Fedoroff, N. V. & Brown, D. D. *Cell* **13**, 717–725 (1978).
76. Erdmann, V. A. *Nucleic Acids Res.* **8**, r31–r47 (1980).
77. Brownlee, G. G., Cartwright, E. M. & Brown, D. D. *J. molec. Biol.* **89**, 703–718 (1974).
78. Jacq, C., Miller, J. R. & Brownlee, G. G. *Cell* **12**, 109–120 (1977).
79. Miller, J. R. & Melton, D. A. *Cell* **24**, 829–835 (1981).
80. Korn, L. J. & Bogenhagen, D. F. in *The Cell Nucleus* (eds Busch, H. & Rothblum, L.) (Academic, New York, in the press).
81. Gurdon, J. B. *J. Embryol. exp. Morph.* **36**, 523–540 (1976).

ARTICLES

After the deluge: Mediterranean stagnation and sapropel formation

Martine Rossignol-Strick

Laboratoire de Palynologie, Muséum National d'Histoire Naturelle, 61 rue de Buffon, 75005 Paris, France

Wladimir Nesteroff, Philippe Olive & Colette Vergnaud-Grazzini

Département de Géologie Dynamique, Université Pierre et Marie Curie, 4 place Jussieu, 75005 Paris, France

In an East Mediterranean marine core, the upper sapropel begins soon after the start of a global event—a very heavy precipitation which occurred in the equatorial latitudes during the late Glacial–early Holocene. This heavy precipitation in Africa, channelled by the Nile River across 35° of latitude, produced a low-salinity surface layer in the East Mediterranean. In this confined basin, with high bottom salinity, the steep salinity gradient stratified the water column. The stagnant bottom waters triggered the sapropel formation. Cretaceous sapropels in the tropical oceans may result from the same chain of events in warm, humid climates, with contrasting wet-and-dry seasonal rhythm.

THE periodic sedimentation of black, pelagic muds rich in marine organic matter (sapropels) has been described extensively in Quaternary and Neogene cores of the East Mediterranean Sea[1–6].

Sapropel formation involves the establishment of a steep vertical salinity gradient in the water column, initiated by highly saline bottom waters[1] and completed by a low salinity surface layer[3,5,7,8], which prevents thermohaline convection and triggers a stable density stratification[1,3,4]. Stagnant bottom waters are rapidly depleted of oxygen, and this reducing environment preserves the pelagic organic matter. The epipelagic fauna is unusual in abundance, assemblage[2,7–9] and isotopic composition[5,7,10–12], the mesopelagic fauna is normal and the benthic fauna almost disappears[2,8,9,13]. Sapropels occur mostly during Quaternary warming phases, but also during some cool isotope stages[3,5,7,8,14].

As a key to stagnation control, several hypotheses on the origin of the low salinity surface layer have been formulated. The Eurasian ice-sheet meltwater hypothesis[2,3,5,11,15,16] is rejected by our ^{14}C data of the most recent sapropel, 11,760–7,950 yr BP: its flushing into the Mediterranean, through the Bosphorus, ended too early, around 13,500 yr BP (ref. 17). It may have lowered the sea surface salinity, but that did not trigger stagnation.

The local Mediterranean increased rainfall hypothesis[1,2,5], is not supported by pollen data (Fig. 1): in Greece and south-west Turkey, the warming trend started around 10,600 BP, and was probably accompanied by a small increase in moisture which became significant only after 8,200 yr BP (refs 18–20). Further south, in Crete[21], moisture increased around 9,500 and after 10,000 yr BP in Syria[22], where warming occurred at 11,500 yr BP.

0028–0836/82/020105—06$01.00

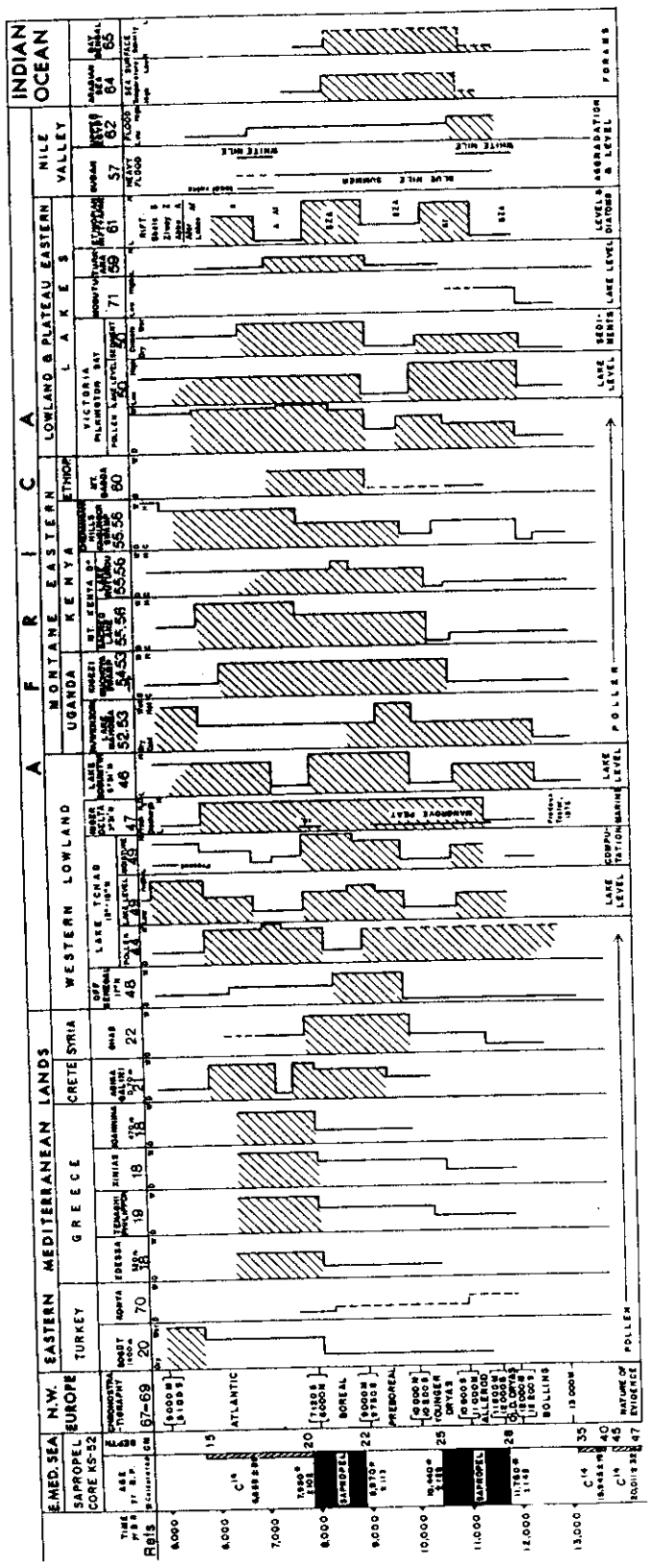

Fig. 1 Chronological setting for sapropel formation, East Mediterranean and African precipitations, Indian Ocean events. Hatched zones indicate the wettest periods.

Around 11,000 yr BP, winters had a very low insolation in the Northern Hemisphere[23], therefore it is unlikely that warmer winter temperatures might have prevented the convective sinking of the Mediterranean surface waters[2]. Downwelling now occurs in winter only in the North Adriatic Sea and around Rhodes[24]. Before stagnation, the marked contrast in seasonal insolation activated the thermohaline convection, with summer evaporation and winter downwelling.

The hydrological isolation of the deep waters in the confined East Mediterranean basin[24] progressively increased their salinity[1]. Stagnation occurred only when the surface water density became appreciably lower than the bottom water[1]. The unusual bottom fauna associated with presapropel layers reflects this increasing bottom salinity as oxygen saturation declines when salinity increases.

Precise dating of the most recent sapropel and isotopic and palynological analysis of its hydrological context suggest that it was the spreading over the sea surface of a low density, low salinity layer of great Nile River floods which triggered total deep-water stagnation. This high-nutrient discharge channelled the precipitation of a very wet period in equatorial Africa into the Mediterranean.

Dating and ^{18}O and ^{13}C isotope analysis

Core Medor 75-KS52 from the Levantine Basin (Fig. 2) (Strabo Trench, south-east of Crete, isolated from Crete by ridges, 34°00′ N–26°19′ E, water depth 3,118 m) displays the upper sapropel from 20 to 28 cm core depth. This is interrupted by a grey nanno-ooze oxygenated layer from 22 to 25 cm (ref. 13). The sapropel overlies a grey hemipelagic nanno-ooze (proto-sapropel) (40–28 cm) and is topped by a light brown nanno-ooze (20–0 cm).

We have established ^{14}C dates from bulk carbonates above and below the sapropel (Table 1). The absence of detrital material >63 μm does not suggest contamination by older carbonates. Since compensation occurs between the −400 yr apparent age resulting from the ^{14}C 50‰ excess in marine organisms compared with terrestrial vegetals (from the ^{13}C 25‰ enrichment of the former), and the +500 yr apparent age resulting from the ^{14}C 60‰ depletion of marine dissolved C, no correction has been applied to the measured ^{14}C age[25,26]. Assuming a constant sedimentation rate, a linear age–depth regression indicates a mean sedimentation rate between 2.0 and 2.3 cm yr^{-1}. Moreover, the isotopic stratigraphy of this core points to the rapid transition Younger Dryas–Preboreal, which took place sometime between 10,500 and 10,000 yr BP (ref. 27), at core depth 25–24 cm, precisely during the sapropel interruption.

Based on the two bracketing ^{14}C dates and the 10,000 yr BP transition, a linear interpolation yields calculated ages of the two-layered sapropel of 11,760 ± 142 to 10,440 ± 129 yr BP, and 8,970 ± 113 to 7,950 ± 102 yr BP. Although the generally accepted age has been 9,000–7,000 yr BP (refs 3, 14), our chronology is strongly supported by our isotopic stratigraphy.

$^{18}O/^{16}O$ and $^{13}C/^{12}C$ ratios of the epipelagic foraminifera *Globigerinoides ruber* are presented in an unprecedently tight sampling of 34 levels in 50 cm of core length in Fig. 3. Oxygen isotopic compositions decrease overall by 3.75‰, from about 17,000 yr BP (40 cm core depth), through several large shifts, to minimal values reached between 8,000 and 6,000 yr BP (21–17 cm). This 3.75‰ decrease ought to correspond to the Termination I continental warming and melting of the northern ice sheet. However, it occurs here over 9,000–11,000 yr, which is much too long. Moreover, it displays three main phases:

(1) A stepwise decrease averaging 2‰ between 40 and 28 cm (17,000–11,800 yr BP) before sapropel deposition (at 28 cm) but including several sharp oscillations of about 1‰ amplitude after 14,000 yr BP. The very high, sharp depletion peak at 28 cm, is 1.5‰ higher than the previous average level, immediately before the beginning of sapropel.

(2) From around 11,000 yr BP to around 10,000 yr BP, a return to values slightly higher than at 17,000 yr BP. They

Table 1 Upper sapropel ^{14}C dates in Mediterranean cores

Ref.	Core	Sediment	Depth (cm)	Age (^{14}C yr BP)
72	Alb-194	Sapropel mud	9–17	8,330 ± 130
73	V10-64	Carbonate in sapropel:	23.5–28.5	
		coarse fraction		8,700 ± 1,000
		fine fraction		7,400 ± 200
		organic matter		8,400 ± 250
74	24M067	Sapropel		7,900 ± 170
75	OT 26	Varved layer	174–178	8,210 ± 185
	OT 25	Under finely laminated layer	core basis	9,640 ± 150
14	P6510-4	Organic ooze above sapropel	21–28	6,575 ± 160
		Sapropel (50–63 cm)	51–60	8,215 ± 160
		Hemipelagic mud below	101–110	10,475 ± 140
This work	KS 52	Nanno-ooze above sapropel-S1	15–20	6,659 ± 89 CRG 97
		Nanno-ooze below sapropel-S1	35–40	15,945 ± 196 CRG 98
		Nanno-ooze	45–47	20,011 ± 323 CRG 99

appear during sapropel deposition and precede ~600 yr the deposition of the intercalated oxygenated ooze, during which the maximum $\delta^{18}O$ is reached. This interval of high values is synchronous with the Younger Dryas cold event (11,160–10,000 yr BP).

(3) A second large, rapid decrease of 3.75‰ before deposition of the younger part of the sapropel, until minimal values are reached between 8,000 and 6,000 yr BP. A subsequent increase of ~1.4‰ leads to present day (average) values, which appear in the upper 10 cm.

^{13}C depletions correlate with minimal $\delta^{18}O$ values at 28.5 and 23.5 cm, but this species displays a rather strong non-equilibrium fractionation[28].

Palaeoclimatic implications

The East Mediterranean basin thus experienced a slow and complicated isotopic transition from glacial stage 2 to postglacial stage 1. The overall 3.75‰ $\delta^{18}O$ variation is more than double the 1.7‰ normal difference between glacial stage 2 and present-day values. The 2.05‰ additional difference is too large to signal only a temperature increase, which would be an excessive +10 °C. A 2–3 °C increase is generally accepted in the Mediterranean during Termination I[5,8], accounting for a $\delta^{18}O$ of −0.7‰. The remaining 1.35‰ has to be accounted for by fresh water influx forming a low salinity surface layer[5,7,10,11].

Moreover, both ^{13}C and ^{18}O isotope depletions occur rapidly before sapropel deposition. A simple calculation shows that the isotopic composition of the fresh water entering the Mediterranean has to be higher than −10‰. This low estimate suggests that precipitation and river discharge are the dominant source of the surface brackish water layer, and not ice sheet meltwater, which would have an isotopic composition around −30‰. River floods started around 12,500 yr BP (second half of the first decrease), waned around 11,000 yr BP, and reappeared immediately after 10,000 yr BP.

The earliest 2.5‰ $\delta^{18}O$ decrease (45–30 cm), dated 20,000–12,600 yr BP, is accounted for by three elements: part of the 1.7‰ global isotopic effect, the 2–3 °C temperature rise, and some salinity decrease due, until 13,500 yr BP, to meltwater influx through the Bosphorus. Partial stagnation developed, resulting in the grey protosapropel layers. Sapropel formation was triggered, after a 230-yr time lag, by the second, sharp, highest 1.5‰ $\delta^{18}O$ depletion, (30–28 cm) between 12,600 and 11,700 yr BP, entirely a salinity effect due to heavy floods.

The Nile River is the only contender for such a discharge. Before the Aswan High Dam construction, Nile flood water was partly carried eastward along the Israeli coast, where it flowed as a 15-m thick surface layer, decreasing the salinity from its normal values of 38.8‰ to 31.80‰ in September[29]. Local rainfall from December to March decreases the salinity only to 36‰ (ref. 30). The Nile flood does not seem to exert a temperature effect[30]. Present-day mean weighted isotopic values of precipitation at Entebbe, Uganda, is −2.91‰ (ref. 31). The freshwater discharge becomes brackish when mixed by winds, currents and internal waves with the seawater. The Nile origin of the brackish surface layer accounts for the frequently observed east–west gradient of decreasing stagnation and surface productivity in the sapropels. A 10% decrease (from 38‰ to 34–35‰) of the surface salinity is sufficient to induce water stratification. Today, stable stratification is observed seasonally in the open tropical oceans where the freshwater discharge of large rivers spreads as a brackish surface layer (<50 m deep), sometimes as far as several hundred kilometres. Stratification from monsoonal discharge occurs in the Andaman Sea, caused by the Irrawady[32], off the West Coast of India with the runoff from the Ghats[33], and from non-monsoonal (zenithal) discharge, in the West Equatorial Atlantic under the influence of the enormous Amazon flow, which sends isolated lenses of brackish water as far as Barbados[34]. In all these cases, a 2–4‰ vertical salinity gradient in the upper 50 m is responsible for the density stratification, whereas the generally warm temperature has little effect on the pycnocline.

The present day Amazon discharge (75 times the Nile), would cover the entire Mediterranean Sea with a 3-m deep freshwater layer in one year[34]. If the late Glacial Nile discharge was 2.5 times larger than today, like the present Zambeze, it could have accumulated a 25-m deep freshwater surface layer over the Levantine and Ionian basins in only 15 yr. The lags we see in the core between the two sets of heavy floods and sapropel incipience are 230 and 800 yr.

The very rapid 3‰ $\delta^{18}O$ increase from 28 to 26.5 cm (11,000–10,000 yr BP) is a result of the cumulative effects of the Younger Dryas glacial buildup, the colder temperatures, and the dramatic decrease of Nile floods, resulting from the simultaneous period of aridity in equatorial Africa. This arid episode is clearly seen in many African low lake levels and pollen diagrams (Fig. 1). It occurred even though the very high incoming summer insolation[23] could have been expected to promote heavy tropical rainfall. The insolation effect in this case is overrun by the atmospheric cooling of high-latitude origin. Colder temperatures in the Mediterranean area are reflected in the Macedonian pollen diagram (zone Y3)[19].

The sharp 3‰ $\delta^{18}O$ depletion from 24.5 to 23.8 cm took place in about 300 yr. It is much too large and rapid to be caused solely by ice melt and warming of the Younger Dryas–Preboreal transition[27]. It signals a salinity lowering due to resumption of heavy Nile floods after 10,000 yr BP. They correlate with the African main rainy period from 10,000 to 8,000 yr BP which builds the highest lake levels around 9,500 yr BP (Fig. 1).

The second half of the sapropel is a consequence of these floods. The time lag between the high floods and sapropel incipience is ~800 yr, which is much longer than the previous one, because the floods discharged over a much more saline sea surface.

In the shallower East Mediterranean core GA32, the bottom-to-surface $\delta^{18}O$ gradient increases suddenly at two levels, suggesting a two-step flooding sequence[12]. The isotopic variation related to salinity change is also 1–1.5‰ here.

Although high nutrient input and planktonic productivity are associated today with the arrival in September of the tongue of Nile flood water off the Israeli coast[30,31,35], one should not argue that the low $^{13}C/^{12}C$ ratios in surface waters are caused by a higher nutrient input. (Each plankton net haul yields 3 cm^3 of

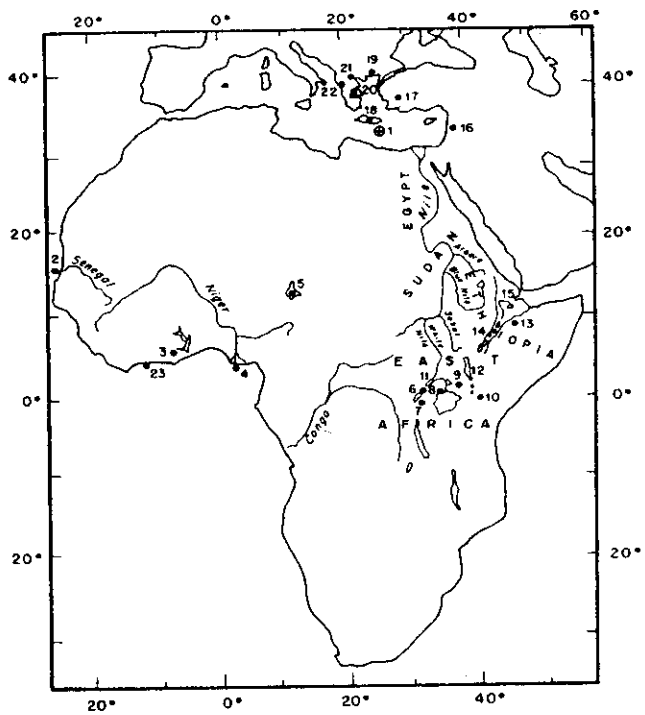

Fig. 2 Location of core and mentioned sites. 1, Core KS52. 2, Core off the Senegal River mouth. 3, Lake Bosumtwi, Ghana. 4, Core off the Niger River mouth. 5, Lake Tchad. 6, Ruwenzori, Lake Mahoma. 7, SW Uganda, Muchoya Swamp. 8, Lake Victoria, Pilkington Bay. 9, Cherangani Hills. 10, Mt Kenya, Sacred Lake, Lake Rutundu. 11, Lake Mobutu Sese Seko (Albert). 12, Lake Turkana (Rudolf). 13, Mt Badda. 14, Ethiopian Rift Lakes. 15, Afar Lakes. 16, Ghab Valley, Syria. 17, Sogüt, Anatolia. 18, Aghia Gallini, Crete. 19, Tenaghi Philippon, Macedonia. 20, Xinias Lake. 21, Edessa. 22, Ioannina. 23, Ivory Coast littoral.

plankton in August, 30–35 cm^3 in September; the yearly average is 4.7 cm^3 and the spring bloom reaches only 12.5 cm^3 (ref. 31).) In the Indian Ocean, the $\delta\ ^{13}C$ of shallow dwelling foraminifera is not related to nutrient supply of upwelling origin[36]. High primary productivity might even be the cause of a higher $\delta\ ^{13}C$ of the ΣCO_2 at the same depths (J. C. Duplessy, personal communication). Thus, the depletion we measure in core KS52 are related to the influx of organic rich freshwaters (with a low $^{13}C/^{12}C$ ratio of the ΣCO_2) of continental origin. These low surface ratios result in an intense vertical $\delta\ ^{13}C$ gradient in the water column.

Pollen

The upper sapropel pollen spectrum (pollen sum 356) (around 9,500 yr BP) predominantly reflects a Mediterranean (48.2%) and warm temperate (6.5%) vegetation. It is very similar to the earliest Holocene in Macedonia (Zones Z1 and 2, 10,300–9,000 yr BP)[19]. An open (herbaceous: 45.4%) oak (31.1%) pine (15.1%) forest occupied the Greek and Turkish Mediterranean shores, and broad-leaved trees (6.5%) requiring more summer moisture grew higher on the slopes. Littoral or desert halophytes (11.1%) were more abundant here than in Macedonia. The cold steppe *Artemisia* is hardly present (6.0%). The pollen is transported by wind to the sea surface, then dispersed by currents as a pelagic element[37]. Well specified Nilotic pollen[38] is absent: the Nile water does not appear to carry pollen further than its sedimentary load; they are only found in Nile silt[38]. The low density characteristic of the Nile water is thus preserved far beyond the silt and pollen deposition limits. The geological implication is that bottom waters in a deep or shallow basin may become anoxic under the influence of fluvial discharge even if the local climate reflected by pollen cannot feed such rivers, and even where clastic sediments do not reach. In fact, bottom anoxicity may occur whatever the lithology of the depositing sediment, provided distance from the continent is not too great. Moreover, this limiting factor can be enlarged in a globally warm climate like the Cretaceous, during which weak winds and sluggish ocean currents do not enhance water mixing.

Late Glacial–early Holocene equatorial deluge

During the last Glacial maximum (19,000–13,000 yr BP), extreme aridity spread in the tropics. It was immediately followed, during the late Glacial–early Holocene (Alleröd–Preboreal–Boreal), by an equatorial heavy rainfall period of global scale, recorded by pollen, in northern South America (Guantiva Interstadial)[39], the Galapagos[40,41], most probably New Guinea[42], with extensive wet Lower Montane *Nothofagus* forest, Sumatra[43], and the Indian Ocean and Africa. Raised lake levels are also conspicuous. It was the wettest period of the past 20,000 yr.

The formation of the Mediterranean sapropel results from a link (the Nile River) across 35° lat. between this climatic event in equatorial Africa and the marine hydrology. The relevant data are shown in Fig. 1.

In Africa, from west to east, and within 10° N of the Equator, the highest precipitation is recorded between 12,500 and 8,000 yr BP. In West Africa, data are from the southern drainage area of Lake Tchad[44], the Ivory Coast mangrove peat[45], the level of Lake Bosumtwi in Ghana[46], and the Niger River discharge[47]. North of 10° N, the onset of the rainy period is delayed. The mangrove along the Senegal River lower course (17° N) thrives after 9,600 yr BP (ref. 48), and the high level of Lake Tchad (13–15° N)[49] and its wettest vegetation[44] occur after 8,500 yr BP.

In East Africa, where the Nile watershed is situated, reinterpreted pollen data from the mountains, 3 °S–2 °N, correlate aridity before 12,000 yr BP with a cool climate, and moisture thereafter with a warm climate[50,51]. On the Ugandan (Ruwenzori, Kigezi[52–54]) and Kenyan (Mt Kenya, Cherangani Hills[55,56]) mountains, the shift towards a wetter and warmer vegetation

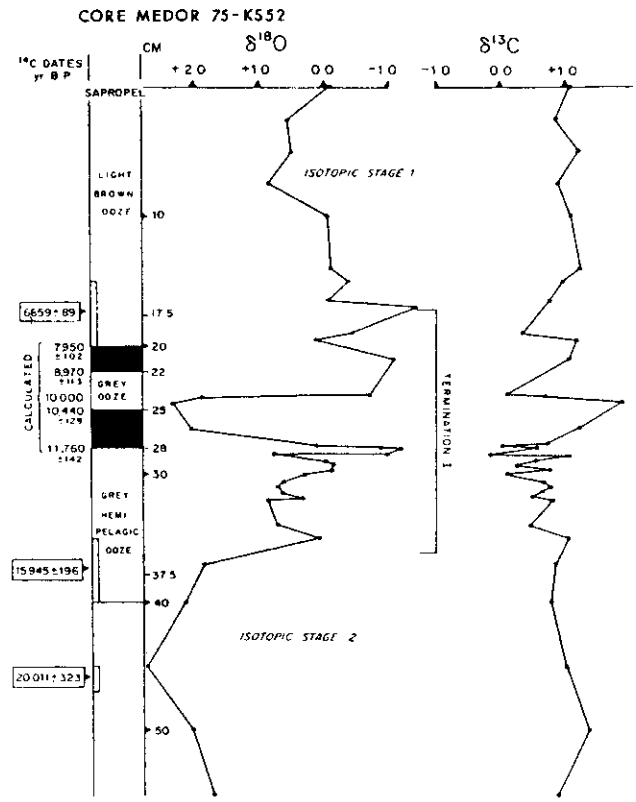

Fig. 3 Sapropel age, ^{18}O and ^{13}C isotopes stratigraphy in core KS52.

belt, of different types according to the altitude of the site, started as early as 12,700 yr BP and developed around 10,800 yr BP. The warmest and wettest local vegetation is usually installed around 8,000 yr BP.

In the lowlands around Lake Victoria, the moisture increased after 12,500 yr BP, and the wettest climate is signalled between 9,500 and 7,000 yr BP by the vegetation, the lake level and its sediments[50]. A widespread dry spell, synchronous with the Younger Dryas, is recorded between 10,800 and 9,500 yr BP in the low levels of Lakes Bosumtwi, Tchad and Victoria, as well as in the vegetation around Lake Victoria and on Mt Kenya.

Before 12,000 yr BP, the Main Nile was dry most of the year, the meagre summer flow fed only by the weak Ethiopian monsoon. After 12,000 yr BP, the East African bi-seasonal rainfall was higher and the White Nile became a very large permanent river, well regulated by the lakes[51,57,58]. Its catchment area was expanded from 9,500 to 7,500 yr BP by the inclusion of the much higher, larger Lake Turkana[59].

Wetter conditions occurred on the southeastern Ethiopian Plateau at Mt Badda, after 11,500 yr BP or possibly only 9,500 yr BP (ref. 60).

Drained by the Blue Nile and the Atbara, the northern Ethiopian Highlands (10–13° N) are inaccessible, but their palaeoclimate is documented by the peripheral Rift and Afar Lakes[61]. The lake levels were highest, much above today, and they merged between 9,500 and 8,500 yr BP. The Ethiopian summer flood of the Nile was therefore much heavier. This seasonal variation accounts for the lamination of the sapropels: the white laminae are formed by coccoliths[14] blooming with the flood, rich in dissolved ions of Ethiopian basalt origin.

The Nile Valley aggradation records these floods mostly from 12,000 to 11,000 yr BP, and from 8,000 to 7,000 yr BP in Sudan and Upper Egypt[57,58,62]. There, aggradation indicates a "wild Nile with aberrant summer floods of a phenomenal volume"[62]. Moreover, higher local Sudanese (15° N) rainfall, which may have reached 550 mm yr^{-1} (163 today)[63], between 8,000 and 7,000 yr BP (ref. 57), suggests decreased evaporation along the course of the Nile. Today, evaporation in the Sudanese swamps heavily reduces the Nile discharge.

The African and Indian monsoons, of equatorial westerlies origin, both controlled by the continental heat trough, displayed the same peak when the summer insolation was higher than today around 11,000 yr BP. At that time, strong monsoonal air flow and high rainfall in India is suggested by low sea-surface summer temperature in the Arabian Sea[64], due to strong upwelling induced by the southwesterly air flow, a mangrove much more extensive than today on the Indian coast near Bombay (E. Van Campo, personal communication), and river discharge higher than today in the Bay of Bengal[65]. The Intertropical Convergence of the tropical easterlies, with its zenithal rains, was reactivated in East equatorial Africa.

From the eastern tropical Atlantic to the Bay of Bengal, along the inner tropics of the African continent and Indian Ocean, and in the other equatorial longitudes, as the summer insolation was highest, the late Glacial–early Holocene was a very wet period, the most humid of the past 20,000 yr. From around 12,500 yr BP, during the Bolling–Alleröd interstadial, the higher rainfall belt migrated progressively from the Equator polewards through the Preboreal and Boreal. The Atlantic was the wettest period in the 50–55° N lat. zone. It was set back by a drier episode which corresponds to the cold Younger Dryas, recorded in the Mediterranean sapropel by the disappearance of the brackish surface layer, thus interrupting the stagnation from 10,400 to 9,000 yr BP.

Conclusion

The Mediterranean two-layered upper sapropel in core KS52 is dated at 11,800–10,400 yr BP and 9,000–8,000 yr BP, the interruption resulting from the Younger Dryas cold/dry event. This is too late to be caused by the influx of Eurasian ice-sheet meltwater. Instead, oxygen and carbon isotope variations in planktonic foraminifera show that the light, low-salinity, organic and nutrient rich sea-surface layer which spread slightly before sapropel deposition and selectively increased the planktonic productivity, originated as rainfall. The pollen record around the eastern Mediterranean does not indicate much increased local rainfall at that time. Meanwhile, in equatorial Africa, very heavy rainfall began at 12,500 yr BP and culminated between 10,000 and 8,000 yr BP. We conclude that this equatorial deluge, channelled by the Nile River over 6,700 km is, as already suggested[58,66], the source of the surface brackish-water layer in the Mediterranean. This layer enhanced the vertical salinity and density gradient, and established stable stratification. Thus bottom stagnation was triggered in this hydrographically restricted deep basin, and sapropel formation resulted. The East Mediterranean behaved as an ectogenic meromictic lake as a stratified estuary and as a fjord during the stagnation events.

The establishment of these climate links have far-reaching geological implications.

(1) The Quaternary climatic chronology of Africa is recorded in the eastern Mediterranean subsurface. Sapropels are formed during all the periods of high summer insolation of the Northern Hemisphere displayed by the Milankovitch curve, which occur even during glacial isotopic stages 3, 4 and 6. The isotope stratigraphy supports these correlations.

(2) Widespread marine stagnation events occurred during certain short and well-defined periods of the Cretaceous. They deposited pelagic laminated sapropels and we suggest that they result from the same chain of events as this recent Mediterranean sapropel. In equatorial West Gondwana around the opening Atlantic, the thick fluvio-deltaic sediments of the Barreirinhas Basin suggest great river discharge in a seasonally very humid tropical climate, with a contrasting dry season enhancing evaporation. These Cretaceous sapropels may be important as possible petroleum generating environments.

Cruise Medor 75 was supported by the Centre National pour l'Exploitation des Oceans, France. The European Economic Community provided research funds. Support was by the CNRS, France. Revision of an earlier version of the manuscript and comments by J. C. Duplessy are acknowledged. We thank L. Burckle, R. Fairbanks, A. Gordon, F. McCoy, A. McIntyre, W. B. F. Ryan for helpful discussions and R. M. Cline for editorial assistance.

Received 8 June; accepted 28 October 1981.

1. Kullenberg, B. *Göteborgs K. Vetensk.-O. Vitterh Samh. Handl.* **B6**, 3–37 (1952).
2. Olausson, E. *Rep. Swedish Deep-Sea Expn 1947–8* **8**, 5, 287–334 (1960); **8**, 6, 337–391 (1961).
3. Ryan, W. B. F. in *The Mediterranean Sea* (ed. Stanley, D. J.) 149–169 (Dowden, Hutchinson & Ross, Stroudsburg, 1972).
4. McCoy, F. W. thesis, Harvard Univ. (1974).
5. Vergnaud-Grazzini, C., Ryan, W. B. F. & Cita M. B. *Mar. Micropaleont.* **2**, 353–370 (1977).
6. Kidd, R. B., Cita, M. B. & Ryan, W. B. F. *Init. Rep. DSDP Leg* **42**, 1, 421–443 (U.S. Govt Print. Off., Washington, 1978).
7. Cita, M. B. *et al. Quat. Res.* **8**, 205–235 (1977).
8. Thunell, R. C., Williams, D. F. & Kennett, J. P. *Mar. Micropaleont.* **2**, 371–388 (1977).
9. Parker, F. L. *Rep. Swedish Deep-Sea Expn. 1947–48* **8**, 2, 217–283 (1958).
10. Vergnaud-Grazzini C. & Herman-Rosenberg Y. *Rev. Geogr. Phys. Geol. Dyn.* **11**, 279–292 (1969).
11. Williams, D. F., Thunell, R. C. & Kennett, J. P. *Science* **201**, 252–254 (1978).
12. Luz, B. *Nature* **278**, 847–848 (1979).
13. Pastouret, L. *Bull. Mus. Anthrop. Prehist.* **16**, 155–171 (Monaco 1970).
14. Stanley, D. J. & Maldonado, A. *Nature* **266**, 129–135 (1977).
15. Ryan, W. B. F. & Cita, M. B. *Mar. Geol.* **23**, 197–215 (1977).
16. Thunell, R. C. & Lohmann, G. P. *Nature* **281**, 211–213 (1979).
17. Grosswald, M. G. *Quat. Res.* **13**, 1–32 (1980).
18. Bottema, S. thesis, Univ. Gröningen (1974); in *The Environmental History of the Near and Middle East since the Last Ice Age* (ed. Brice, W. C.) 15–28. (Academic, New York, 1978).
19. Wijmstra, T. A. *Acta bot. neerl.* **18**, 511–527 (1969).
20. Van Zeist, W., Woldring, H. & Stapert, D. *Palaeohistoria* **17**, 53–143 (1975).
21. Bottema, S. *Rev. Palaeobot. Palynol.* **31**, 193–217 (1980).
22. Niklewski, J. & Van Zeist, W. *Acta bot. Neerl.* **19**, 737–754 (1970).
23. Berger, A. L. *Quat. Res.* **9**, 139–167 (1978).
24. Lacombe H. & Tchernia, P. *Cah. Oceanogr.* **12**, 527–547 (1960).
25. Broecker, W. S. & Gerard, R. *Limnol. Oceanogr.* **14**, 883–888 (1969).
26. Broecker, W. S. *J. geophys. Res.* **84**, 3218–3225 (1979).
27. Lowe, J. J., Gray, J. M. & Robinson, J. E. *Studies in the Late Glacial of North West Europe* (Pergamon, Oxford, 1980).
28. Duplessy, J. C., Bé, A. W. H. & Blanc, P. L. *Palaeogeogr. Palaeoclimatol. Palaeoecol.* **33**, 9–46 (1981).
29. Hecht, A. *Bull. Sea Fish. Res. Sta. Haifa, Israel* **36**, 24 pp (1964).
30. Liebman, E. *Rapp. P.-v. Réun. Comm. int. Explor. scient. Mer Mediterr.* **9**, 181–186 (1935).

31. Statistical Treatment of Environmental Isotope Data in Precipitation *Tech. Rep., Ser.* 206, (IAEA, Vienna, 1981).
32. Ramesh Babu, V. & Sastry, J. S. *Ind. J. mar. Sci.* **5**, 179–189 (1976).
33. Wyrtki, K. *Oceanographic Atlas of the International Indian Ocean Expedition* (National Science Foundation, Washington, 1971).
34. Ryther, J. H., Menzel, D. W. & Corwin, N. *J. mar. Res.* **25**, 69–83 (1967).
35. Halim, Y. *J. Cons. perm. int. Explor. Mer* **26**, 57–67 (1960).
36. Prell, W. L. & Curry, W. B. *Oceanol. Acta* **4**, 91–98 (1981).
37. Rossignol-Strick, M. *Init. Rep. DSDP Leg* **13**, 971–991 (1973).
38. Rossignol, M. *Notes Mém Moyen-Orient* **10**, 1–272 (1969).
39. Van Geel, B. & Van der Hammen, T. *Palaeogeogr. Palaeoclimatol. Palaeoecol.* **14**, 9–92 (1973).
40. Colinvaux, P. A. *Nature* **240**, 17–20 (1972.
41. Colinvaux, P. A. & Schofield, E. K. *J. Ecol.* **64**, 989–1012 (1976).
42. Hope, G. S. *J. Ecol.* **64**, 627–663 (1976).
43. Maloney, B. K. *Nature* **287**, 324–326 (1980).
44. Maley, J. *X INQUA Congr. Suppl. Bull. AFEQ* **1**, 50, 187–197 (1977).
45. Fredoux, A. & Tastet, J. P. *7th Africa Micropaleont. Colloq.* Ile-Ife, Nigeria (1976).
46. Talbot, M. R. & Delibrias, G. *Earth planet. Sci. Lett.* **47**, 336–344 (1980).
47. Pastouret, L., Chamley, H., Delibrias, G., Duplessy, J. C. & Thiede, J. *Oceanol. Acta* **1**, 217–232 (1978).
48. Rossignol-Strick, M. & Duzer D. *Pollen Spores* **21**, 105–134 (1979).
49. Servant M. & Servant-Vildary, S. *Palaeoecol. Afr.* **6**, 87–92 (1972); in *The Sahara and the Nile* (eds Williams, M. A. J. & Faure, H.) 133–172 (Balkema, Rotterdam 1980).
50. Kendall, R. L. *Ecol. Monogr.* **39**, 121–176 (1969).
51. Livingstone, D. A. *A. Rev. Ecol. System.* **6**, 249–280 (1975).
52. Livingstone, D. A. *Ecol. Monogr.* **37**, 25–52 (1967).
53. Hamilton, A. in *East African Vegetation* (eds Lind, E. M. & Morrison, E. S.) 188–209 (Longman, London 1974); *Palaeoecol. Afr.* **7**, 45–149 (1972).
54. Morrison, M. E. S. *Nature* **190**, 483–486 (1961); *J. Ecol.* **56**, 363–384 (1968).
55. Coetzee, J. A. *Nature* **204**, 564–566 (1964); *Palaeoecol. Afr.* **3**, 1–146 (1967).
56. Van Zinderen Bakker, E. M. & Coetzee, J. A. *Palaeoecol. Afr.* **7**, 151–181 (1972).
57. Williams, M. A. J. & Adamson, D. A. *Nature* **248**, 584–586 (1974); in *The Sahara and the Nile* (eds Williams, M. A. J. & Faure, H.) 281–304 (Balkema, Rotterdam, 1980).
58. Adamson, D. A., Gasse, F., Street, F. A. & Williams, M. A. J. *Nature* **288**, 50–55 (1980).
59. Butzer, K. W., Isaac, G. L., Richardson, J. L. & Washbourn-Kamau, C. *Science* **175**, 1069–1076 (1972).
60. Hamilton, A. C. *X INQUA Congr. Abs. Birmingham* 193 (1977).
61. Gasse, F., Street, F. A. *Palaeogeogr. Palaeoclimatol. Palaeoecol.* **24**, 279–325 (1978).
62. Butzer, K. W. in *The Sahara and the Nile* (eds Williams, M. A. J. & Faure, H.) 253–280 (Balkema, Rotterdam 1980).
63. Wickens, G. E. *Boissiera* **24**, 43–65 (1975).
64. Prell, W. L. in *Evolution des Atmosphères planétaires et Climatologie de la Terre*, 149–156 (CNES Colloq. Int., Nice, 1978).
65. Cullen, J. L. *Geol. Soc. Am. San Diego Meet. Abstr.* 408 (1979).
66. Nesteroff, W. D., Olive, P., Rossignol-Strick, M. & Vergnaud-Grazzini, C. *P. V. CIESM-17 Congr. Cagliari* (1980).
67. Shotton, F. W. in *British Quaternary Studies, Recent Advances* (ed. Shotton, F. W.) 17–29 (Clarendon, London 1977).
68. Mangerud, J., Andersen, S. T., Berglund, B. E. & Donner, J. J. *Boreas* **3**, 109–127 (1974).
69. Mangerud, J., Larsen, E., Longva, O. & Sonstegaard, E. *Boreas* **8**, 179–187 (1979).
70. Roberts, N., Erol, O., de Meester, T. & Uerpmann, H. P. *Nature* **281**, 662–664 (1979).
71. Livingstone, D. A. in *The Sahara and the Nile* (eds Williams, M. A. J. & Faure, H.) 339–359 (Balkema, Rotterdam, 1980).
72. Olsson, J. *Am. J. Sci., Radiocarbon Suppl.* **1**, 87–102 (1959).
73. Olson, E. A. & Broecker, W. S. *Am. J. Sci. Radiocarbon Suppl.* **3**, 141–175 (1961).
74. Pastouret, L. *Tethys* **2**, 227–266 (1970).
75. Fabricius, F. H., Von Rad, U., Hesse, R. & Ott, W. *Geol. Rdsch.* **60**, 164–192 (1970).

Polyoma virus capsid structure at 22.5 Å resolution

I. Rayment, T. S. Baker & D. L. D. Caspar

Rosenstiel Basic Medical Sciences Research Center, Brandeis University, Waltham, Massachusetts 02254, USA

W. T. Murakami

Department of Biochemistry, Brandeis University, Waltham, Massachusetts 02254, USA

X-ray diffraction data from polyoma capsid crystals were phased by refinement of low-resolution starting models to obtain a self-consistent structural solution. The unexpected result that the hexavalent morphological unit is a pentamer shows that specificity of bonding is not conserved among the protein subunits in the icosahedrally symmetric capsid.

X-RAY crystallographic studies on polyoma virus were begun to visualize the protein subunit packing in the icosahedral capsid and to explore the way in which the chromatin core of this tumorigenic virus is packaged inside its protein shell[1]. Analysis of electron micrographs has established that the capsid consists of 12 five-coordinated and 60 six-coordinated morphological units[2] (capsomeres) arranged on a $T = 7d$ icosahedral surface lattice[3] (Fig. 1). It has been presumed, based on the principles formulated to account for the morphology and chemical composition of simple icosahedral virus particles[4], that the capsids of the $T = 7$ papova viruses should be constructed from 420 identical protein subunits quasi-equivalently bonded into 12 pentameric and 60 hexameric capsomeres. High-resolution X-ray structure determination of tomato bushy stunt virus[5] and southern bean mosaic virus[6] has established that quasi-equivalence is used to conserve essential bonding specificity among the 180 chemically identical subunits of these $T = 3$ icosahedral capsids. Our 22.5-Å resolution electron density map of the polyoma capsid reveals unexpected substructure in the hexavalent capsomere that is inconsistent with the expectation of quasi-equivalent bonding of identical subunits. (The adjectives 'hexavalent' and 'pentavalent' are introduced to identify the six- and five-coordinated morphological units without prejudging the nature of their substructure.)

The starting point for our analysis of the polyoma capsid diffraction data was a model representing the coarse surface features seen in the three-dimensional image reconstruction from electron micrographs of negatively stained particles[3]. The capsomeres in this image reconstruction appear as hollow, stubby protrusions with no regular substructure, about 50 Å in diameter and separated from their nearest neighbours by 80–90 Å at a radius of 200 Å in the capsid. Pentavalent and hexavalent morphological units appear to be about the same size, which would not be expected if they were composed of pentamers and hexamers of identical protein subunits.

Cells infected with polyoma virus and other papova viruses produce, in addition to intact virions and empty capsids, hollow tubular particles that appear to be polymorphic assemblies of the capsomeres[7]. There are two categories of tube: wide tubes,

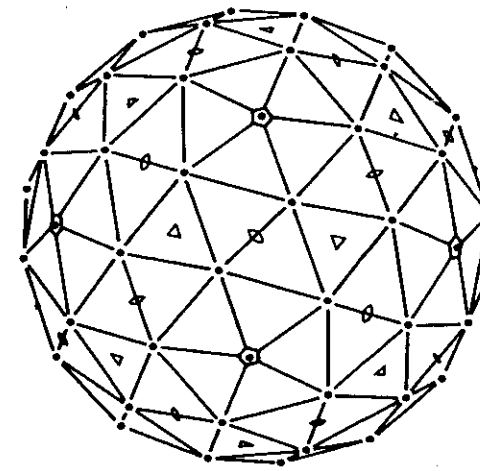

Fig. 1 $T = 7d$ icosahedral surface lattice with five-, three- and two-fold axes marked. The drawing shows one side of the polyhedral surface consisting of 60 six-coordinated and 12 five-coordinated lattice points at the same radius. The location of the six-coordinated point is that determined for the hexavalent morphological unit in the polyoma capsid.

0028-0836/82/020110—06$01.00

expansion could be the factor that triggered the formation of the Laurentide ice sheet[28]. However, the results of our experiment are only preliminary as with only 2 yr of simulation their statistical significance cannot be firmly established. A significance-testing formula[29] will be needed which requires several additional years of simulation, followed by a comparison with results from higher-resolution models. To explain the subsequent growth of the ice sheet, other factors not considered in this simulation, such as the albedo feedback and modifications of oceanic circulation[30,31], will have to be included in the model. Other simulations with more realistic surface conditions for the different phases of the ice sheet build-up will be necessary to analyse in detail the mechanisms responsible for the complete transition to glacial conditions.

We thank A. Berger for his suggestion that we should undertake this work and for many helpful discussions.

Received 4 February; accepted 11 May 1983.

1. Berger, A. *Vistas Astr.* **24**, 103–122 (1980).
2. Shaw, D. M. & Donn, W. L. *Science* **162**, 1270–1272 (1968).
3. Suarez, M. & Held, I. M. *J. geophys. Res.* **84**, 4825–4836 (1979).
4. North, G. R. & Coakley, J. A. *J. atmos. Sci.* **36**, 1189–1204 (1979).
5. Schneider, S. H. & Thompson, S. L. *Quat. Res.* **12**, 188–203 (1979).
6. Birchfield, G. E., Weertman, J. & Lunde, A. T. *J. atmos. Sci.* **39**, 71–87 (1982).
7. Berger, A. *Astr. Astrophys.* **51**, 127–135 (1976).
8. Imbrie, J. *Icarus* **50**, 408–422 (1982).
9. Wetherald, R. T. & Manabe, S. *J. atmos. Sci.* **32**, 2044–2059 (1975).
10. Mason, B. J. *Q. Jl R. met. Soc.* **102**, 473–498 (1976).
11. Kutzbach, J. E. & Otto-Bliesner, B. L. *J. atmos. Sci.* **39**, 1177–1188 (1982).
12. Berger, A. *Il Nuovo Cimento* **2C**, 63–76 (1979).
13. Shackleton, N. J. & Matthews, R. K. *Nature* **268**, 618–619 (1977).
14. Shackleton, N. J. *Proc. R. Soc.* **B174**, 135–154 (1969).
15. Ruddiman, W. F. & McIntyre, A. *J. geophys. Res.* **82**, 3877–3887 (1977).
16. Ruddiman, W. F. & McIntyre, A. *Science* **204**, 173–175 (1979).
17. Alexander, R. C. & Mobley, R. L. *Mon. Weath. Rev.* **104**, 143–148 (1976).
18. Phillips, N. A. *J. Met.* **14**, 184–185 (1957).
19. Bourke, W. *Mon. Weath. Rev.* **102**, 688–701 (1974).
20. Orszag, S. A. *J. atmos. Sci.* **27**, 890–895 (1970).
21. Hoskins, B. J. & Simmons, A. J. *Q. Jl R. met. Soc.* **101**, 637–655 (1975).
22. Rodgers, C. D. *Q. Jl R. met. Soc.* **93**, 43–54 (1967).
23. Slingo, J. *Q. Jl R. met. Soc.* **106**, 747–770 (1980).
24. Kuo, H. L. *J. atmos. Sci.* **31**, 1232–1240 (1974).
25. Bhumralkar, C. M. *J. appl. Met.* **14**, 1246–1258 (1975).
26. Berger, A. *J. atmos. Sci.* **35**, 2362–2367 (1978).
27. Williams, L. D. *Quat. Res.* **10**, 141–149 (1978).
28. Andrews, J. T. & Mahaffy, M. A. W. *Quat. Res.* **6**, 167–183 (1976).
29. Chervin, R. M. & Schneider, S. *J. atmos. Sci.* **33**, 405–412 (1976).
30. Johnson, R. C. & Andrews, J. T. *Quat. Res.* **12**, 119–134 (1979).
31. Ruddiman, W. F., McIntyre, A., Niebler-Hunt, W. & Durazzi, J. T. *Quat. Res.* **13**, 33–64 (1980).

African monsoons, an immediate climate response to orbital insolation

Martine Rossignol-Strick

Laboratoire de Palynologie, Faculté des Sciences USTL, 34000 Montpellier, France, and Lamont-Doherty Geological Observatory, Columbia University, Palisades, New York 10964, USA

The Croll–Milankovitch astronomical theory of climate[1–3] has received strong support from the evidence of a linear climatic forcing by obliquity and precession, although nonlinearity had to be assumed for eccentricity[4,5]. Moreover, interglacials have appeared to be controlled by the orbital insolation[6] although a phase shift of 6,000–5,000 yr is seen between an astronomical climate index and terrestrial climate indicators, dominated by the northern ice-sheet dynamics. Climate proxy data of low latitudes are less directly dependent on the ice sheets. Here it is shown that during the past 464,000 yr, African monsoons signalled by the East Mediterranean sapropels were heaviest always and only when a northern summer monsoon index, computed from the orbital variation of insolation, reached maximum values. This occurred during all the interglacials, but also twice during glacial periods. Thus tropical aridity is not the single climatic pattern of glacial periods. An immediate terrestrial climate response to orbital variations of insolation is established.

Heavy monsoons in Africa have been recorded by the black organic-rich layers called sapropels in the subsurface of the East Mediterranean Sea, a consequence of heavy discharge[7] from the Nile River. I show here that they responded immediately to the variable distribution of northern-summer orbital insolation in time and space, described globally by the astronomical computation during the past 464,000 yr. Run-off from the inaccessible Northern Ethiopian Highlands orographic rains (May to September) produces the Nile River summer flood, 75–80% of the annual average discharge[8]. The annual progress of the mean monthly rainfall in Ethiopia[9] shows that it belongs to the monsoonal Sudanian Zone, with southwesterly winds at 850 mbar at least from June to August[10]. The recent annual rainfall variability is similar in the Highlands, evaluated through the integrating mean Nile River discharge, and in the Sudanian Zone in West Africa. As in most of the tropics, a sudden change occurred in 1898[11], when the mean Nile regime decreased abruptly by 28% (ref. 8). Since 1898, the Nile flow[8,11] and the Sudanian Zone[12,13] have both undergone drought phases in the early 1910s, 1940s and late 1960s to mid-1970s, and relatively wetter phases in the 1930s and 1950s to early 1960s.

During the northern-summer monsoon in Africa[13–15], two synoptic elements are closely correlated with the rainfall variability, while the duration of the rainy season, normal during dry years, lengthens during wet years[13]. First, the amount of rain in the Sudan Zone diminishes when the seasonally migrating 'heat trough' is less marked, pressures being higher than average[13–15]. It increases when the poleward excursion of the trough is larger[13,16,17].

Second, the equatorial westerlies, which straddle the Equator, seem to respond to the steepness of the meridional and longitudinal pressure gradients between the heat trough low pressure and the higher pressure near the cooler Equator[14,15,18–23].

In summer 1972, an extreme large-scale north tropical drought occurred in Africa, Central India, the Caribbean and Venezuela accompanied by a very strong wet El Niño in the south tropics[12,16,17,24–28]. The African heat trough (ITCZ) was not marked, the Equator-to-ITCZ pressure gradient was small, the equatorial westerlies and their associated upper level easterly jets were weak while the low-level tropical easterlies were stronger[16,17,28,29]. Zonally averaged atmospheric temperatures (surface to 100 mbar)[30] were globally below average in 1971, and until summer 1972 at 10–30° N (−0.6 °C), while the Equator (−0.5 °C in 1971) was already above average (+0.2 °C) in summer 1972. This weakened the Equator (cold)–north tropics (warm) temperature gradient in summer 1972. Thus, the extreme drought was accompanied by lower tropical temperature and weaker Tropic–Equator gradient. The Southern Hemisphere temperature gradient was also decreased by above average South Pole temperatures from 1970 to 1975 (+0.4 °C in 1972) and the south oceanic anticyclones were displaced southward[17].

Since 1900, no extremely wet year has occurred in West Africa[11,13]. In the less dry 1958[12,13,26,27], the global mean temperatures were above average in the northern subtropics (+0.6 °C), below at the Equator (−0.7 °C), producing a steeper Equator–Tropic gradient, and average at the South Pole[30].

Based on the previous analysis, the following synoptic situation is proposed for presently unknown very heavy African monsoon: (1) A well marked heat trough, with very low pressures, reaching the Tropic (23°27′ N) in summer. (2) Strong Equator-to-Tropic baroclinicity. The Southern Hemisphere winter baroclinicity, (20–70 °S) reflects the strength of the southern winter trade-winds[10].

To reconstruct the African monsoons of the Quaternary, this prescribed meteorology will be formulated by using the boundary radiative values of orbital insolation during the caloric northern summer half-year[2].

The insolation at the north Tropic I_T reflects the intensity of the heat trough. The latitude of the Tropic shifts by 2°41′

0028–0836/83/270046—04501.00

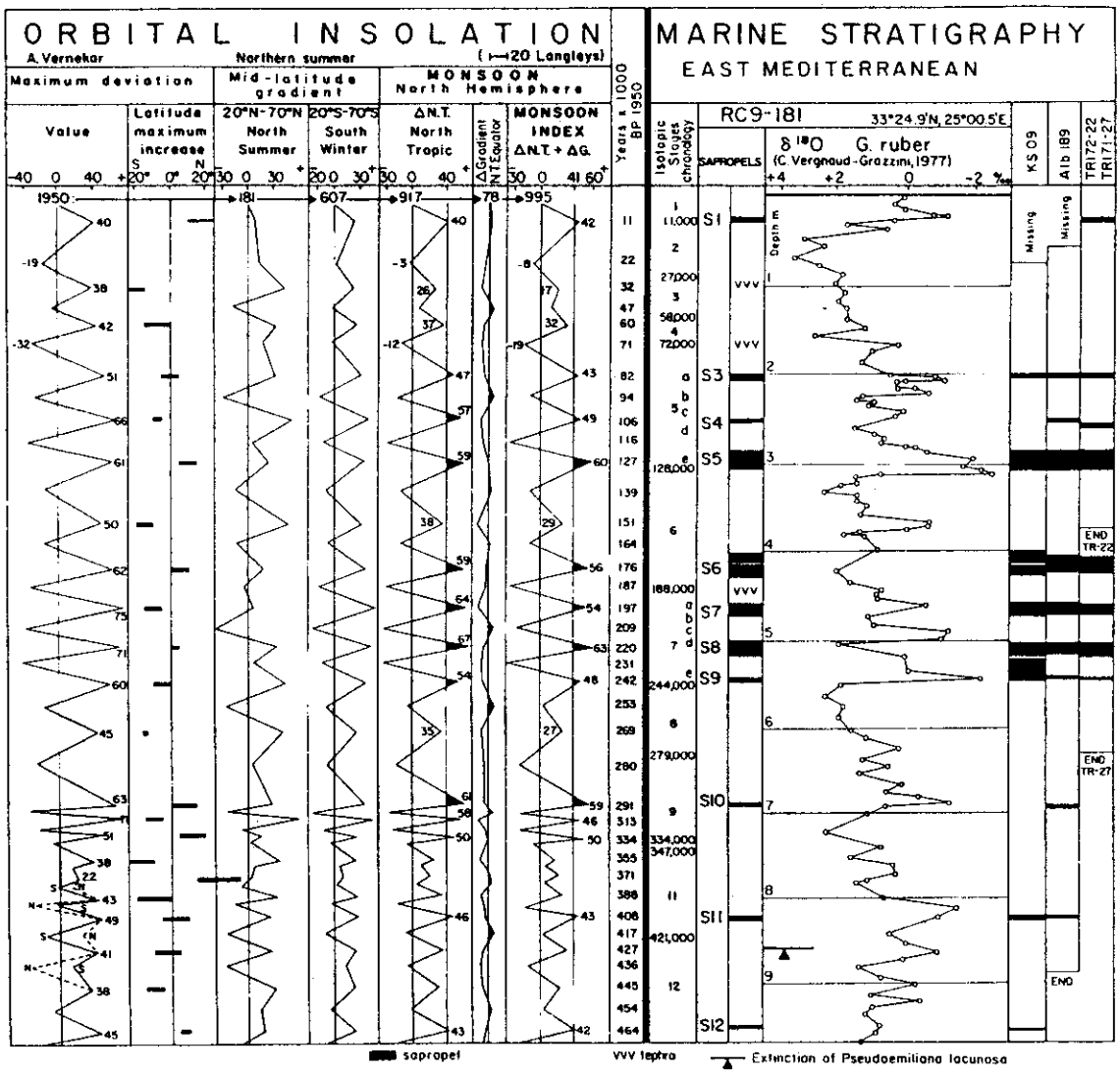

Fig. 1 Correlation of the orbital insolation monsoon index (caloric half year northern summer) with deep-sea sapropels in the East Mediterranean—insolation in langleys (cal cm^{-2}) day-1 in Δ AD 1950. Absolute value of AD 1950 insolation on top line, ref. 2. Isotopic stages chronostratigraphy, ref. 32. Core RC9-181; 33°25′ N, 25°00′ E; 2,286 m ref. 31. Core KS-09; 35°09′ N, 20°09′ E; 2,800 m ref. 34. Core Alb. 189; 33°54′ N, 28°29′ E; 2,604 m, ref. 35. Core Tr 172-22; 35°19′ N, 29°01′ E; 3,150 m, ref. 36. Core Tr 172-27; 33°50′ N, 25°59′ E; 2,680 m, ref. 36. Vertical scale for orbital insolation and isotopic chronostratigraphy based on RC9-181 core depth.

according to the Earth's axis obliquity, with a 41,000-yr period[1-3].

The gradient of insolation I_T–I_E between the north Tropic and the Equator reflects the baroclinicity between these latitudes.

An orbital insolation monsoon index M at time t is established:

$$M' = I_T' + (I_T' - I_E') = 2I_T' - I_E'$$

The variation of M for the past 464,000 yr is shown in Fig. 1. The astronomical time scale is adjusted on the δ^{18}O chronostratigraphy of core RC9-181 in Fig. 1. The Southern Hemisphere winter baroclinicity is described by the 20°–70° S insolation gradient:

$$G_s = I_{20} - I_{70}$$

The insolation values appear as their deviation from the AD 1950 absolute values, shown on the upper line. The periods of highest insolation of the northern summer display the highest monsoon index M, as well as the largest Southern Hemisphere winter gradients.

The East Mediterranean sapropel and δ^{18}O stratigraphy of core RC9-181 (ref. 31) is shown in Fig. 1. The chronostratigraphy of the δ^{18}O stage boundaries[32] establishes the correlation of the Mediterranean marine record with the monsoon index. The extinction of the coccolith *Pseudoemiliana lacunosa*, observed worldwide within stage 12 (ref. 33), has been recognized below sapropel 11 (ref. 31). Reexamination of the core showed that sapropel 2 does not exist (F. McCoy, personal communication).

A sapropel was formed every time the increasing northern summer insolation produced an index M above the threshold value of 41, and no sapropel occurred outside of these periods. The origin of the only exception, 'missing' sapropels in stage 9, has to be investigated. Four other cores with δ^{18}O curve are also shown[34-36]. The epipelagic δ^{18}O depletion events of the Nile floods appear when the sampling interval is very dense[7].

Two physical parameters combine to produce threshold M: the magnitude and the latitude of the insolation maxima, seen in the first two columns of Fig. 1. These maxima have to be higher in the Southern than in the Northern Hemisphere to reach threshold M. At 11,000 yr BP, the maximum was the

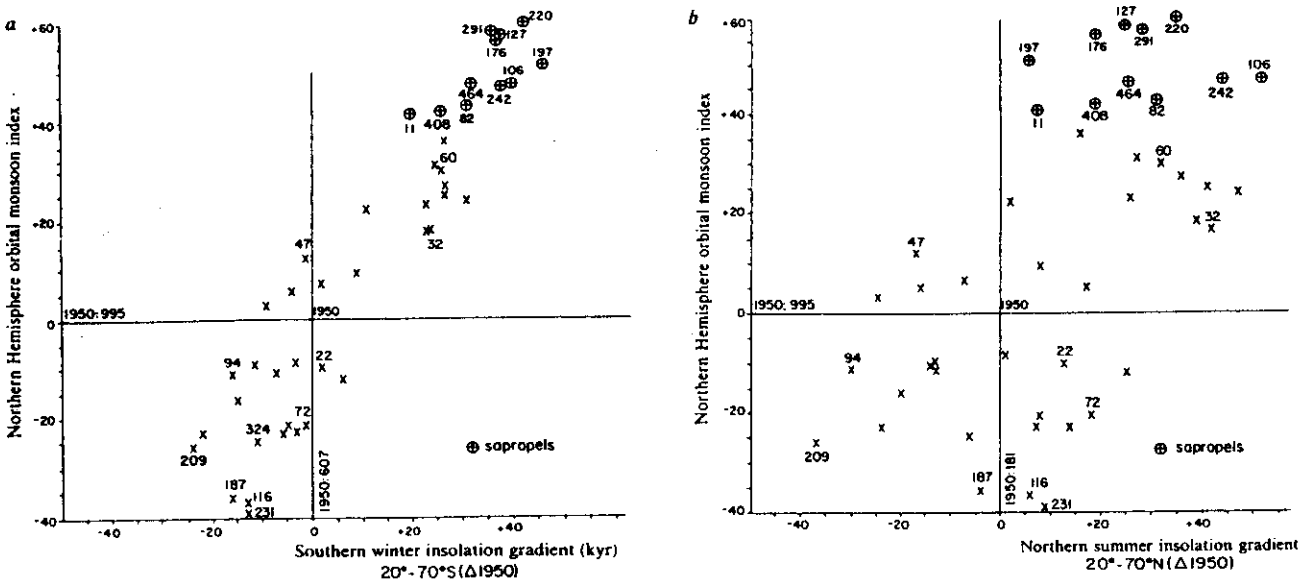

Fig. 2 Northern Hemisphere monsoon index, sapropel formation and *a*, southern winter; *b*, northern summer mid-latitude insolation gradient reflecting the strength of *a*, southern winter *b*, northern summer trade-winds. Insolation as in Fig. 1.

smallest which triggered a sapropel, but it was the furthest north (10–25° N).

The mid-latitude insolation gradient, reflecting trade-wind strength, is controlled by the 20° lat. insolation, since the largest orbital insolation variations occur in the tropics. As seen in Fig. 2, high M and sapropel formation correlate well with the largest insolation gradients of the southern winter, supporting the 1972 drought analysis and Kraus's hypothesis[12], but not with those of the northern summer.

Corresponding to highest M, sapropels deposited most frequently during the warming phases of interglacials[31,34–36]. Northern tropical rainfall in all longitudes was heaviest from 12,500 to 8,000 yr BP (ref. 7), particularly during the Indian monsoon[37–39], successfully simulated at 9,000 yr BP (refs 40, 41). During the 127,000-yr BP Eemian insolation peak, the Indian monsoon also increased[37], and lakes appeared in Libya around 130,000 yr BP (ref. 42). The sapropel pollen record seen in Fig. 3 shows the warm, sub-humid character of the Mediterranean area vegetation during these interglacial sapropels, with high values for trees (*Quercus* and *Pinus*), low for steppe (*Artemisia*).

However, the thick and widespread sapropels S6 and S8 formed during periods with large ice sheets: glacial stage 6, and cold interstadial 7d within interglacial stage 7. Their planktonic fauna was cold[31,34], and their pollen record points to a continental dry Mediterranean climate, with high values for steppe, low for trees. Precisely during these two periods, M was among the highest ever at 176,000 yr BP and 220,000 yr BP, with the insolation peaks centred at 0–10° and 0–5° N lat. Actual trade winds were the strongest ever, enlarged by the tropical warming and the polar ice-sheets cooling. At 220,000 yr BP, highest M followed very abruptly a record low at 231,000 yr BP. At 60° N, the very low June-to-August insolation between 230,000 and 225,000 yr BP (ref. 3), resulted in the voluminous ice-sheet depicted by the previously described[4,43], brief but severe isotopic enrichment of stage 7d.

Thus African tropical aridity during northern glacial periods, as seen at 18,000 yr BP, is not an exclusive climatic pattern. Large northern ice sheets have been coeval with very wet African northern tropics, suggesting that ice-sheet global cooling alone is not able to produce tropical aridity. High local tropical insolation appears therefore as the foremost climatic parameter correlated with heavy African monsoon, and the difference between the tropical aridity around 18,000 yr BP and

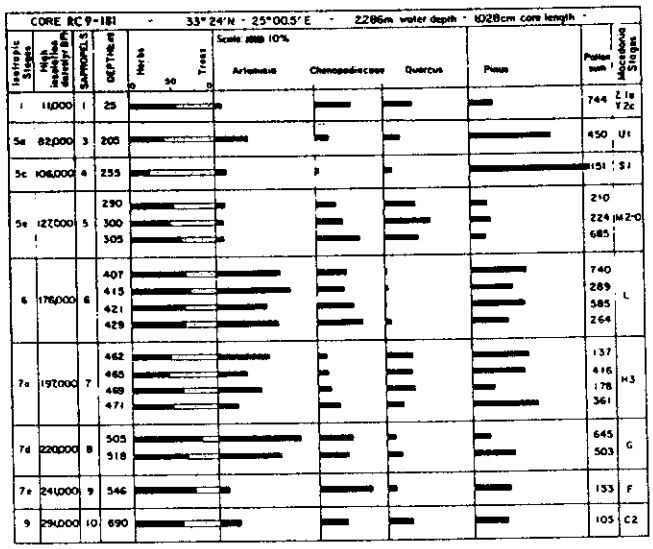

Fig. 3 Elements of pollen spectra of sapropels in Mediterranean core RC9-181. Sapropel numeration as in Fig. 1. Macedonia stages from refs 59, 60.

the 176,000 and 220,000 yr BP heavy monsoons is prominently the tropical insolation.

The north-tropical lowest insolation of 22,000 yr BP, which was only −3 langleys at 25° N, triggered the arid period which lasted until 13,000 yr BP and suggests feed-back processes perpetuating the drought through increased albedo[12,44–46].

During the last glacial, M was always higher than presently from 25,000 to 66,000 yr BP, with minor peaks at 32,000 and 60,000 yr BP. Correspondingly, a wet phase is recorded around and below 30,000 yr BP by sapropels near the Nile mouth[47], around 30,000 yr BP in sub-Saharan Africa[48–52], between 40,000 and 20,000 yr BP in Lake Tchad[53], between 30,000 and 21,000 yr BP in Ethiopian Rift Lakes[54,55], around 36,000 and from 30,000 to 21,000 yr BP in south-west Arabia[56,57].

The strong correlation in the tropics between warm periods and heavy rainfall suggests that in the geological past during

such periods, whatever their cause, heavy precipitation on the continents extended stratified estuarine circulation to continental shelves and oceanic basins, and produced marine organic-rich sediments similar to the Quaternary Mediterranean sapropels, which eventually became petroleum and phosphorite source beds. The same process accounts for the origin of strata-bound ores associated with organic-rich black shales.

M.R.-S. is supported by the Centre National de la Recherche Scientifique, LA327, France. Critical reading of a previous version of this manuscript by J.C. Duplessy, A. McIntyre, W. Ruddiman and M. Van Campo is gratefully acknowledged, as well as conversations with A. Berger, J. Hays, J. Imbrie, G. Kukla, J. Kutzbach, J. Morley, W.B.F. Ryan, and C. Vergnaud-Grazzini, and editorial assistance by R.M. Cline. I thank a reviewer for the suggestion to apply a refinement in time scale and monthly insolation computation, more accurate than in ref. 2, for the period before 200,000 yr BP (ref. 58). This is Lamont–Doherty Geological Observatory contribution no. 3480.

Received 4 February; accepted 29 April 1983.

1. Milankovitch, M. *Acad. Royale Serbie Ed Spec. Vol.* 133 (Sect. Sc. Math et Nat., T. 33, Belgrade, 1941).
2. Vernekar, A. D. *Met. Monogr.* **12** (1972).
3. Berger, A. L. *Quat. Res.* **9**, 139–167 (1978); *Nuovo Cimento* 2C, 163–187 (1979).
4. Hays, J. D., Imbrie, J. & Shackleton, N. J. *Science* **194**, 1121–1132 (1976).
5. Imbrie, J. & Imbrie, J. Z. *Science* **207**, 943–953 (1980).
6. Kukla, G., Berger, A., Lotti, R. & Brown, J. *Nature* **290**, 295–300 (1981).
7. Rossignol-Strick, M., Nesteroff, W., Olive, P. & Vergnaud-Grazzini, C. *Nature* **295**, 105–110 (1982).
8. Riehl, H., El-Bakry, M. & Meitlin, J. *Mon. Weath. Rev.* **107**, 1546–1553 (1979); *Science* **206**, 1178–1179 (1979).
9. Thompson, B. W. *The Climate of Africa* (Oxford University Press, London, 1965).
10. Newell, R. E., Kidson, J. W., Vincent, D. G. & Boer, G. J. *The General Circulation of the Tropical Atmosphere and Interactions With Extratropical Latitudes* Vol. 1 (1972), Vol. 2 (1974) (MIT Press, Cambridge).
11. Kraus, E. B. *Q. Jl R. met. Soc.* **82**, 96–98 (1956).
12. Kraus, E. B. *Mon. Weath. Rev.* **105**, 1009–1018, 1052–1055 (1977).
13. Nicholson, S. E. *Mon. Weath. Rev.* **107**, 620–623 (1979); **108**, 473–487 (1980); **109**, 2191–2208 (1981).
14. Flohn, H. *Bonn. met. Abh.* **5**, 36–48 (1965); **5**, 49–57 (1965); **10** (1969).
15. Flohn, H. & Struning, J. O. *Bonn. Met. Abh.* **15** (1971).
16. Kidson, J. W. *Q. Jl R. met. Soc.* **103**, 441–456 (1977).
17. Krueger, A. F. & Winston, J. S. *Mon. Weath. Rev.* **103**, 465–473 (1975).
18. Lettau, B. *Mon. Weath. Rev.* **102**, 208–214 (1974).
19. Krivelevich, L. M. & Romanov, Y. A. *Soviet Met. Hydrol.* **10**, 32–37 (1980).
20. Semyonov, Y. K. *Arch. Met. Geophys. Bioklim.* B25, 305–321 (1978).
21. Fletcher, R. D. *J. Met.* **2**, 167–174 (1945).
22. Palmer, C. E. *Q. Jl R. met. Soc.* **78**, 126–164 (1952).
23. Frost, R. & Stephenson, P. M. in *Proc. Symp. Tropical Meteorology* (ed. Hutchings, J. W.) 96–105 (New Zealand Meteorological Service, Wellington, 1963).
24. Flohn, H. *Bonn. met. Abh.* **21** (1975).
25. Flohn, H. & Fleer, H. *Atmosphere* **13**, 96–109 (1975).
26. Tanaka, M., Weare, B. C., Navato, A. R. & Newell, R. E. *Nature* **255**, 201–203 (1975).
27. Motha, R. P., Leduc, S. K., Steyeart, L. T., Sakomoto, C. M. & Strommen, N. D. *Mon. Weath. Rev.* **108**, 1567–1578 (1980).
28. Kanamitsu, M. & Krishnamurti, T. N. *Mon. Weath. Rev.* **106**, 331–347 (1978).
29. Newell, R. E. & Kidson, J. W. in *Saharan Dust: Mobilization, Transport, Deposition* (ed. Morales, C.) 133–169 (Wiley, New York, 1979).
30. Angell, J. K. & Korshover, J. *Mon. Weath. Rev.* **103**, 1007–1012 (1975); **105**, 375–385 (1977); **106**, 755–770 (1978).
31. Vergnaud-Grazzini, C., Ryan, W. B. F. & Cita, M. B. *Mar. Micropaleont.* **2**, 353–370 (1977).
32. Morley, J. J. & Hayes, J. D. *Earth planet. Sci. Lett.* **53**, 279–295 (1981).
33. Thierstein, H. R., Geitzenauer, K. R., Molfino, B. & Shackleton, N. J. *Geology* **5**, 400–404 (1977).
34. Cita, M. D. *et al. Quat. Res.* **8**, 205–235 (1977).
35. Emiliani, C. *Quaternaria* **2**, 87–98 (1955).
36. Thunell, R. C., Williams, D. F. & Kennett, J. P. *Mar. Micropaleont.* **2**, 371–388 (1977).
37. Van Campo, E., Duplessy, J. C. & Rossignol-Strick, M. *Nature* **296**, 56–59 (1982).
38. Cullen, J. L. *Palaeogeogr. Palaeoclimatol. Palaeoecol.* **35**, 315–356 (1981).
39. Duplessy, J.-C. *Nature* **295**, 494–498 (1982).
40. Kutzbach, J. E. *Science* **214**, 59–61 (1981).
41. Kutzbach, J. E. & Otto-Bliesner, B. L. *J. atmos. Sci.* **39**, 1177–1188 (1982).
42. Gaven, G., Hillaire-Marcel, C. & Petit-Maire, N. *Nature* **290**, 131–133 (1981).
43. Ninkovitch, D. & Shackleton, N. J. *Earth planet. Sci. Lett.* **27**, 20–34 (1975).
44. Otterman, J. *Science* **186**, 531–533 (1974).
45. Charney, J. G. *Q. Jl R. met. Soc.* **101**, 193–202 (1975).
46. Charney, J. G., Stone, P. & Quirk, W. *Science* **187**, 434–435 (1975).
47. Stanley, D. J. & Maldonado, A. *Nature* **266**, 129–135 (1977).
48. Sonntag, C. *et al. Palaeoecol. Afr.* **12**, 158–171 (1980).
49. Grove, A. T. & Warren, A. *Geogr. J.* **134**, 194–208 (1968).
50. Rognon, P. *Rev. Geogr. Phys. Geol. Dyn.* **18** 251–282 (1976).
51. Rognon, P. & Williams, M. *Palaeogeogr. Palaeoclimatol. Palaeoecol.* **21**, 285–327 (1977).
52. Faure, H. & Williams, M. *Ass. Senegal Et. Quat. Afr. Bull.* **51**, 75–81 (1977).
53. Servant, M. & Servant-Vildary, S. in *The Sahara and the Nile* (eds Williams, M. & Faure, H.) 132–162 (Balkema, Rotterdam, 1980).
54. Street, F. A. *Palaeoecol. Afr.* **12**, 137–158 (1980).
55. Gasse, F. *Palaeoecol. Afr.* **12**, 333–350 (1980).
56. McClure, H. A. *Nature* **263**, 755–756 (1976).
57. Hotzl, H. & Zotl, J. G. in *Quaternary Period in Saudi Arabia* (eds AlSayari, S. S. & Zotl, J. G.) 301–311 (Springer, New York, 1979).
58. Berger, A. *J. atmos. Sci.* **35**, 2362–2367 (1978).
59. Wijmstra, T. A. *Acta bot. neerl.* **18**, 511–527 (1969).
60. Wijmstra, T. A. & Smit, A. *Acta bot. neerl.* **25**, 297–312 (1976).

0028–0836/83/270049—03$01.00

Radiocaesium from Sellafield effluents in Greenland waters

A. Aarkrog*, H. Dahlgaard*, L. Hallstadius†, H. Hansen* & E. Holm†

* Risø National Laboratory, DK 4000 Roskilde, Denmark
† University of Lund, Lasarettet, S 22185 Lund, Sweden

Since the middle of the 1970s, discharges of radiocaesium to the Irish Sea from the British Nuclear Fuels Ltd Sellafield (formerly Windscale) installation in Cumbria have increased the concentrations of ^{137}Cs and ^{134}Cs in the northern North Atlantic. In coastal British waters[1,2] enhanced concentrations have also been seen in the North Sea[3–5], the Danish Straits and western part of the Baltic Sea[4,5], the Norwegian coastal current[6,7], and the Barent and Greenland Seas[7]. We report here that radiocaesium from Sellafield is now detectable in the East Greenland polar current. The transit time from Sellafield is estimated at 6–8 yr. The concentrations in the polar current are approximately one-thousandth of those found in the North Channel by the outlet from the Irish Sea.

In August 1982 groups from Risø National Laboratory and Lund University collected 200-l samples of the surface seawater along the Greenland east coast (see Table 1) using a pump from M/S *Nella Dan*. The radiocaesium was contained in precipitates of 100 g AMP (ammonium molybdophosphate)[8] taken on board and later measured by Ge(Li) spectroscopy for ^{137}Cs. To determine ^{134}Cs it was necessary to concentrate the activity. After being dissolved in NaOH the radiocaesium in 0.5 kg AMP aliquots (representing 1 m^3 of water) was reprecipitated as 0.5 g Cs_2PtCl_6 with a 90% recovery of activity. This procedure improved the measuring geometry and removed ^{228}Ra and ^{228}Ac (γ photon: 794.9 keV), which disturbed the γ measurement of ^{134}Cs (γ photons: 604.7 keV and 795.8 keV) when performed directly on the AMP. The removal of ^{228}Ac was so efficient that both photo peaks of ^{134}Cs gave the same results, and the high resolving power of our Ge(Li) spectrometer meant that it was not necessary to correct for interference from the 609.4 keV peak of ^{214}Bi. The procedure applied had a lower limit of detection for ^{134}Cs of 0.01 Bq m^{-3}.

The mean ^{137}Cs concentration at the five western stations, 5.43 ± 0.08 (± 1 s.e.m.) Bq m^{-3}, was significantly ($P \sim 99\%$) lower than that of the five eastern ones, 6.70 ± 0.38 Bq m^{-3}. The ^{134}Cs concentration was 0.043 Bq m^{-3} at the eastern and 0.012 Bq m^{-3} at the western stations.

Fallout from nuclear-weapons testing in the atmosphere is the main source of ^{137}Cs in the oceans. To determine the 'non-Sellafield' contribution of ^{137}Cs in the samples we utilized our measurements of surface seawater collected at Danmarkshavn (76°49′ N, 18°36′ W) and Angmagssalik (65°35′ N, 37°52′ W) during 1978–80 [9]. Östlund[10] has found that "the average age of the freshwater component is 11 ± 1 yr from its first appearance at the shelf to its emergence from the basin as a constituent of the modified Atlantic (Arctic) water in the East Greenland current". Both Danmarkshavn and Angmagssalik are situated in the polar current respectively north and south of our sampling stations. This residence time of ~11 yr is compatible with our own ^{90}Sr and ^{137}Cs observations in surface seawater collected annually at Danmarkshavn and Angmagssalik since 1963.

The time constant λ for the decrease of ^{137}Cs in the polar current is the sum of the radioactive decay constant for ^{137}Cs, λ_{Cs} ($= \ln 2/30.5$ yr^{-1}), and the time constant for the freshwater component in the Arctic Ocean is λ_{AO} ($= 1/11$ yr^{-1}).

$$\text{Hence } \lambda = 0.023 + 0.091 = 0.114 \text{ yr}^{-1}$$

which corresponds to an effective half life of ^{137}Cs in the polar current of $\ln 2/0.114 = 6.1$ yr.